Biochimica et Biophysica Acta, 986 (1989) 172–186
Elsevier

BBAMEM 74643

The cardiac sodium channel shows a regular substate pattern indicating synchronized activity of several ion pathways instead of one

Wolfgang Schreibmayer [1], Helmut A. Tritthart [1] and Hansgeorg Schindler [2]

[1] *Institute for Medical Physics and Biophysics, Universität Graz, Graz and* [2] *Institute for Biophysics, Universität Linz, Linz-Auhof (Austria)*

(Received 15 March 1989)

Key words: Sodium ion channel; Cardiac muscle; Toxin; S-DPI 201-106; ATX II; Veratridine

Cardiac sodium channel substates were induced by using different gating modifiers, namely S-DPI 201-106 (s), toxin II from *Anemonia sulcata* (a), veratridine (v) and mixtures of these agents (s + v, a + v). Current ratios (normalized substate currents), slope conductances, reversal potentials and saturation characteristics were evaluated for the individual channel substates. The results can be summarized as follows: (i) Current ratios fell into a pattern of six equidistant values (I to VI) irrespective of the modification applied (0.20, 0.34, 0.51, 0.69, 0.85, 1.00). Slope conductances, determinable for substates II, V and VI (4.8, 11.7 and 14.0, respectively), are also consistent with six conductance substates which are integer multiples of a smallest conductance (state I). (ii) The permeability ratio P_{Na^+}/P_{K^+} (i.e., reversal potential of substate currents) of the sodium channel was conserved both for different modifications, i.e., by s, a, s + v and a + v, and for the different substates (at least for II, IV and VI) observed for each modification. (iii) Sodium binding to the channel is substate independent. Analysis of slope conductances of states II and VI for three sodium chloride concentrations (71.5, 140 and 303 mM) revealed different maximal conductances ($g_{eVImax} = 2.9 \cdot g_{eIImax}$) but similar apparent affinities for sodium ($K_{Na^+VI} = 286$ mM; $K_{Na^+II} = 303$ mM). These findings are shown to seriously challenge the commonly unquestioned conception that 'single-current events' reflect ion passage through only one single pathway. The alternative view, that not one pore, but either six or three pores with synchronized gating ('oligochannel') underlie 'single-channel events', is shown to readily account for the observed substate properties and appears not to contradict known properties of 'the sodium channel'. This fundamentally new view of the sodium channel aims to invoke further efforts to distinguish between conceptually distinct models of structure-function relationships for a variety of channels which show multiple substates and conserved ion selectivity.

Introduction

Early studies of ion channels in their native membrane environment (patch clamp) described in most cases only one open state for a given channel (Neher and Sakmann [1], Horn and Patlak [2], Sigworth and Neher [3], Horn et al. [4]). Multiple open states in isolated ion channel events were first observed in artificial bilayer membranes (Schindler and Rosenbusch [5], Schindler and Rosenbusch [6], Latorre and Alvarez [7]). Since these early studies, evidence for multiple open states has accumulated in both patch-clamp and artificial membrane studies for several channel types (for a partial review see Fox [8]). For the electrically excitable sodium channel under normal physiological conditions, however, only sparse evidence exists so far for the occurrence of open channel substates (Cachelin et al. [9] and Kunze et al. [10]). The infrequency of these observations is probably due to the short open time of sodium channels and their small current amplitudes, which render resolution of open channel substates difficult. Therefore, these results have been interpreted more in terms of different sodium channel populations. Recently, however, using improved substate resolution techniques, clear evidence for sodium channel substates has been provided (Patlak [11]). Sodium channels treated with different gating modifiers, on the other hand, often exhibited reduced single-channel conductance (Quandt et al. [12], Yoshii and Narahashi [13], Chinn and Narahashi [14]). Neuroblastoma cell sodium channels, treated with gating modifiers, exhibited up to five different

Correspondence: W. Schreibmayer, Institute for Medical Physics and Biophysics, Universität Graz, Harrachgasse 21/IV, A-8010 Graz, Austria.

current levels through the open channel (Nagy [15]). Up to now, no mechanistic aspects have been deduced from such substate behaviour, and no physiological role has been assigned. The aim of our study was to induce subconductance states in cardiac sodium channels by modifiers and mixtures of them, namely S-DPI 201-106 (s), toxin II from *Anemonia sulcata* (a) and veratridine (v). Current ratios, slope conductance, selectivity and saturation of sodium translocation were measured for individual channel substates. The results are discussed in terms of current concepts of ion permeation through sodium channels.

Part of this study has been presented in poster form at the 11th Meeting of the Working Group on Cardiac Cellular Electrophysiology in Amsterdam, Autumn 1987.

Material and Methods

Cell preparation

Ventricular cardiomyocytes from adult rats (180–250 g) of either sex were isolated and cultured as described earlier (Schreibmayer et al. [16]). The cells were kept for short-term culture in an incubator for 4 to 72 h. Immediately before electrophysiological experiments were performed, the cells were transferred to a petri dish, the temperature of which could be controlled by means of a Peltier element. Controlled micromanipulations (MO-103, Narishige, Japan; patch clamp tower, List Medical Instruments, F.R.G.) in this dish were possible under the view of an inverted microscope (Zeiss IM 35, F.R.G.). The cells were allowed to settle to the bottom of the petri dish for several minutes, then the cells were washed with extracellular solution to remove culture medium and cell debris. After complete exchange of solutions in the cell bath, single-channel recordings were performed.

Single-channel recordings

Single-channel currents were recorded with the patch-clamp method (Hamill et al. [17]) in the cell-attached configuration at 20 °C. Glass pipettes (American Glass Co.; Glass 7740, square i.d.) with a resistance ranging between 10 and 20 megaohms (standard pipette solution) were used. Sylgard coating was not required for effective analog capacitance transient compensation. Single-channel currents were amplified with a List LM/EPC-7 patch-clamp amplifier (List Medical, FRG) and stored on PCM tape (Sony PCM 501 ES, modified according to Bezanilla [18] and Panasonic Video Cassette Recorder NV-430). Sodium channel currents were elicited by hyperpolarizing the membrane-patch relative to the resting membrane potential and subsequent suprathreshold depolarizing voltage pulses, which were supplied by an arbitrary waveform generator (Wavetek 275, U.S.A.), or by setting the patch potential to the desired value (steady-state recordings).

Evaluation of single-channel records

The current traces were replayed from tape and sampled continuously by the analog to digital converter of an HP 1000 A900 minicomputer (Hewlett Packard) at rates between 1 and 5 kHz and stored on the disk drive.

Before being digitized, the analog signal was filtered by a lowpass Bessel filter at a frequency that was half the sampling rate of the analog to the digital converter. By means of a digital trigger algorithm, the continuous datafile was cut into smaller individual records for further processing. From a set of current records resulting from a given voltage jump, individual records that did not contain any single-channel openings were selected and averaged. These averaged 'blank'-records were subtracted from all records to compensate digitally for residual capacitance currents. These corrected records (all records resulting from a given patch potential) were digitally lowpass filtered (Gaussian type) and then single-channel current-amplitudes were measured by means of a cursor on a digital graphical display (HP 1347A). Whole records or segments of records were plotted by a digital plotter (Rikadenki RY-101).

Statistical analysis of data was done with the statistical graphics package ('Statgraphics') from Statistical Graphics Corporation.

Solutions

The composition of the electrolyte solutions used was as follows (in mM):

Extracellular solution. Na^+: 140; K^+: 5.4; Ca^{2+}: 2.0; Mg^{2+}: 2.0; Cl^-: 153.4; glucose: 10.0; Hepes: 10.0 buffered to pH 7.4.

Standard pipette solution was the same as the extracellular solution containing in addition 1 mM $BaCl_2$ to block inward potassium currents. For certain experiments two other NaCl concentrations are used (303 and 71.5 mM) as specified in Results. For 71.5 mM NaCl, 68.5 mM choline chloride was added for compensation of the osmolarity.

Chemicals

Collagenase for cell disaggregation was purchased from Worthington (Type CI-28). Toxin II from *Anemonia sulcata* (ATX-II) and veratridine were purchased from Sigma Chemicals (Munich, F.R.G.). S-DPI 201-106 was from Sandoz (Basel, Switzerland). All other chemicals used were reagent grade.

Results

Presentation of results is ordered with respect to effects of different Na^+-channel ligands or their combinations on elementary sodium current events. For each ligand (x) or ligand pair (x + y) isolated elementary sodium current events (I_e^x or I_e^{x+y}), i.e., single events

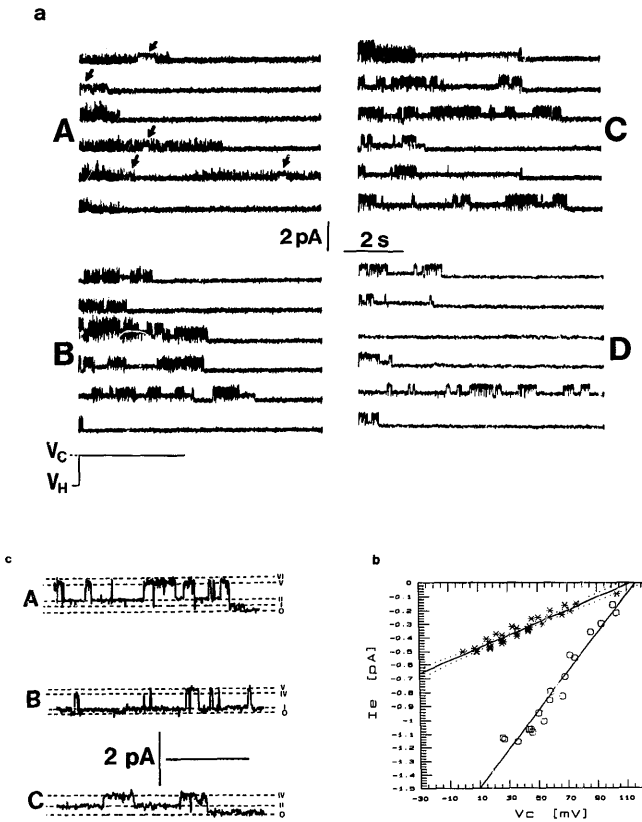

Fig. 1. Sodium currents at 140 mM NaCl through cardiac sodium channels modified by S-DPI (100 μM) and veratridine (10 μM). (a). Traces were obtained by keeping the membrane patch for 25 s hyperpolarized relative to the resting membrane potential ($RP - V_H$) and then stepping the potential to $RP - V_C$ (A: $V_H = +48$ mV, $V_C = -9$ mV; B: $V_H = +49$ mV, $V_C = -18$ mV; C: $V_H = +49$ mV, $V_C = -27$ mV; D: $V_H = +49$ mV, $V_C = -36$ mV). Current records were digitized at a sample frequency of 1 kHz and digitally lowpass filtered (LP) at 250 Hz. RP could not be measured directly as the cell-attached configuration was used. (b). Current-voltage relationships for level II (•) and level VI (○). Slope conductances were calculated by linear regression analysis (95% confidence interval): $g^{s,\uparrow}_{all}{}^{V} = 4.7 \pm 0.6$ pS (mean ± standard error (S.E.), correlation coefficient: 0.96); $g^{s,\uparrow}_{sVI}{}^{V} = 14.2 \pm 0.8$ pS, correlation coefficient: 0.97. (c). Selected current events that showed further sublevels in addition to the main levels II and VI. Lines through definite sublevels were drawn by hand and numbered as stated in Results. LP was 100 Hz. V_C values and time bars (Δt) of the traces were: A: −27 mV, 2.4 s; B: −43 mV, 2.6 s; C: −44 mV, 0.8 s.

occurring between intervals of zero current, are analyzed in terms of resolvable sublevel structure. For the altogether six discernable sublevels we use the nomenclature I^{s}_{el} to I^{s}_{eVI}, where index I refers to the smallest and index VI to the largest sublevel current observed.

Sodium channels modified by a S-DPI and veratridine mixture (index s + v)

140 mM Sodium chloride. In nine different cell attached membrane patches effects of an S-DPI/veratridine mixture on sodium channels were analyzed by observing currents during repetitive hyper- and depolarization of the patch. As can be seen from Fig. 1a A–D, isolated sodium current events (I_e^{s+v}) fluctuated frequently between two resolvable sublevels, designated as I_{el}^{s+v} and I_{eVI}^{s+v}. At lower depolarization (Fig. 1a A) the lower level I_{el}^{s+v} was well discernable in individual records (see arrows in part A). With increasing depolarization (from A to D in steps of 9 mV from RP) a second higher level, designated as I_{eVI}^{s+v}, became resolvable due to increased open times with increasing depolarization. The slope conductances of these two main current levels, i.e., g_{el}^{s+v} and g_{eVI}^{s+v}, were estimated by linear regression and turned out to be 4.7 ± 0.6 pS and 14.2 ± 0.8 pS (mean $\pm$ standard error (S.E.)), respectively (see Fig. 1b).

From the traces we conclude that the two main levels, II and VI, correspond to sublevels of identical Na^+ channels rather than to two populations of channels with different conductances. In several aspects the occurrence of the two levels is correlated: In single events there are direct transitions between 0 (closed) and VI as well as transitions between II and VI. The probability for such transitions in overlapping events of two independent types of channels would be close to zero. Also, additive levels (II + VI) are seen only in obviously overlapping events (third trace in Fig. 1a B), but not in single events. This provides clear evidence that the two levels originate from the same conducting unit assuming different conductance levels and not from two different types of channels *.

In the altogether 279 records evaluated (for which Fig. 1a shows representative traces) a few further sublevels were observed, but only rarely. They are indicated in Fig. 1c in three selected traces. Unfortunately, the relative occurrence of these sublevel events was too sparse for meaningful determination of slope conductances and was as follows: I_{el}^{s+v}: two events in the 279 records examined (0.7%), I_{elI}^{s+v}: 5 (1.8%), I_{elV}^{s+v}: 7(2.5%) and I_{eV}^{s+v}: 11 (3.9%). So instead of comparing level conductances we can only provide estimates for current levels, which expressed as fractions of the current of level VI read: 0.17–0.23, 0.23–0.33, 0.46–0.54, 0.62–0.72, 0.76–0.90, for levels I to V.

Thus, using the modifier pair S-DPI/veratridine we observe six different channel conductance states, numbered from I to VI with increasing conductance, where states II and VI are by far the most populated ones.

303 mM Sodium chloride. At 303 mM sodium, the gating behaviour of the S-DPI/veratridine modified channel was virtually unchanged and again sublevels II and VI were dominant. Fig. 2a shows representative traces for 760 evaluated records derived from six different cell attached membrane patches. Depolarization voltages increase from parts A to D of the figure. Slope conductances were calculated by linear regressions to be 8.7 ± 0.3 pS and 24.5 ± 1.7 pS for levels II and VI, respectively (see Fig. 2b). Ten events with sublevel IV were observed in 1.3% of all records. The distribution at different pipette potential values allowed calculation of g_{elV}^{s+v}, in addition to g_{elI}^{s+v} and g_{eVI}^{s+v}. Linear regression yielded 16.2 ± 1.2 pS for g_{elV}^{s+v} (Fig. 2b).

Sublevels I, III and V could also be detected (I_{el}^{s+v}: 60 events (7.9%); I_{elII}^{s+v}: 3 events (0.4%); I_{eV}^{s+v}: 9 events (1.2%)). Fractional currents were: 0.16–0.22, 0.27–0.35, 0.38–0.56, 0.64–0.70, 0.78–0.88, for I_{el}^{s+v} to I_{eV}^{s+v}, normalized to I_{eVI}^{s+v}. Selected fluctuations of sublevel currents are shown in Fig. 2c. Opening to the smaller sublevels not only occurred after depolarization but also at hyperpolarizing membrane potenials (see Fig. 2c A).

71.5 mM Sodium chloride. In two different cell attached patches sodium fluxes through S-DPI/veratridine modified channels were registrated at 71.5 mM sodium (Fig. 2d), the lowest salt concentration for substate resolution. The two dominant current levels observed are assigned to be again levels II and VI. The slope conductances of these sublevels have been calculated to be: 3.1 ± 0.9 pS and 9.0 ± 1.8 pS for II and VI, respectively (Fig. 2e). Among the 172 individual records examined there were six sublevel fluctuations to I_{el}^{s+v} (3.5%) and one fluctuation to I_{elV}^{s+v} (0.6%, not shown). The current ratios of the resolved sublevels normalized to I_{eVI}^{s+v} were estimated to be: 0.18–0.28 for I_{el}^{s+v} and 0.34–0.44 for I_{elI}^{s+v}.

Veratridine modified sodium channels (index v)

Effects of only veratridine were investigated at 100 μM concentration on two cell attached membrane patches.

Under steady-state conditions (at constant pipette potential) sodium channel openings could not be detected. Upon repetitive hyper- and de-polarization cycles sodium channel openings were observed. Their conduc-

* During the review process of this paper, Nilius et al. [54] reported on three conductance states of the guinea-pig cardiac sodium channel (5, 8 and 15 pS). These states are roughly equivalent to our states, II, III and VI. On the basis of reduced TTX-sensitivity, Nilius et al. [54] assigned the 5 pS pathway to a separate distinct sodium channel. Due to the strict time-correlation of states II and VI observed by us in our experiments, however, it is clear that our level II is a subconductance state of the fully conducting sodium channel (state VI).

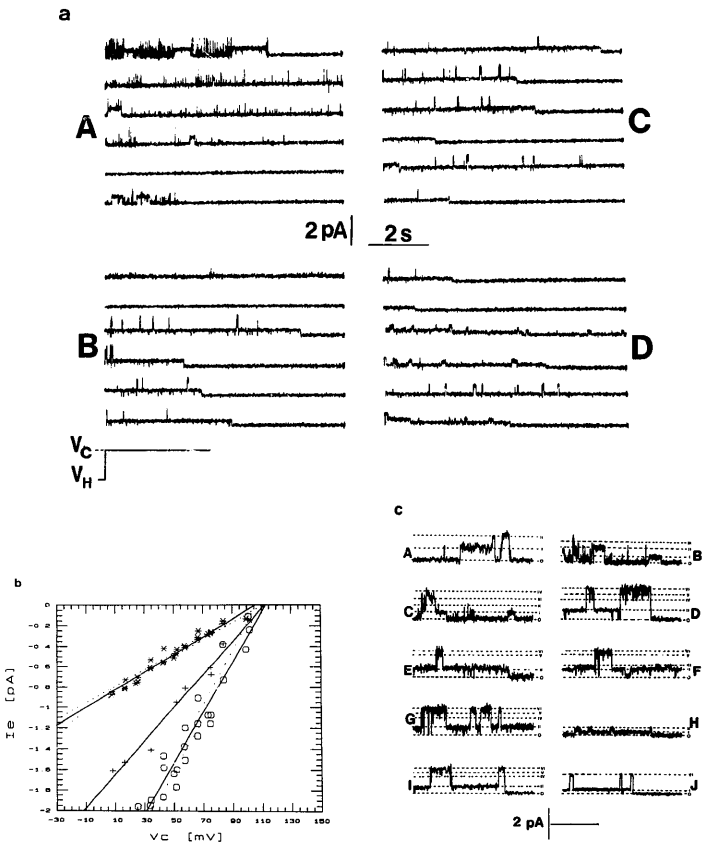

Fig. 2. Sodium currents through S-DPI (200 μM)/veratridine (10 μM) modified sodium channels at different sodium ion concentrations: 303 mM (a-c) 71.5 mM (d, e). (a). V_H and V_C values (defined in the legend to Fig. 1) were: A: $V_H = +42$ mV, $V_C = -26$ mV; B: $V_H = +43$ mV, $V_C = -43$ mV; C: $V_H = +48$ mV, $V_C = -57$ mV; D: $V_H = +50$ mV, $V_C = -75$ mV. Sampling rate was 1 kHz and LP = 250 Hz. (b). Current-voltage relationships for levels II (•), IV (+) and VI (○). $g_{sII}^{s,s} = 8.7 \pm 0.3$ pS, correlation coefficient: 0.98; $g_{sII}^{s,w} = 16.2 \pm 1.2$ pS, correlation coefficient: 0.98; $g_{sVI}^{s,s} = 24.5 \pm 1.7$ pS, correlation coefficient: 0.96. (c). Selected single-event traces showing fluctuations between different channel current sublevels. V_C, LP and Δt values were: A: +45 mV, 1 kHz, 0.2 s; B: −8 mV, 250 Hz, 0.8 s; C: −8 mV, 250 Hz, 0.6 s; D: −35 mV, 250 Hz, 0.32 s; E: −43 mV, 1 kHz, 0.2 s; F: −44 mV, 250 Hz, 0.4 s; G: −44 mV, 1 kHz, 0.36 s; H: −44 mV, 250 Hz, 0.8 s; I: −44 mV, 250 Hz, 0.32 s; J: −58 mV, 100 Hz, 1.32 s. (d). V_H and V_C values were: A: +40 mV, −8 mV; B: +40 mV, −34 mV. Sampling rate was 1 kHz and LP = 100 Hz. (e). Current-voltage relations for levels II (•) and VI (○). Slope conductances $g_{sII}^{s,s} = 3.1 \pm 0.4$ pS, correlation coefficient: 0.95; $g_{sVI}^{s,s} = 9.0 \pm 1.8$ pS, correlation coefficient: 0.92.

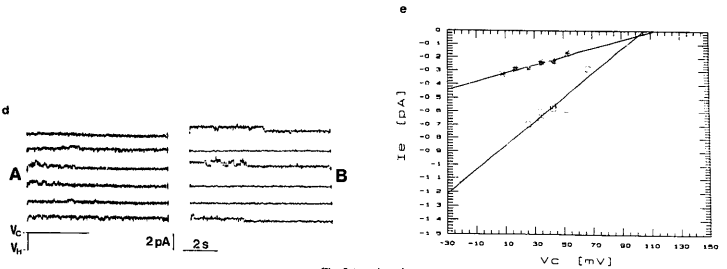

Fig. 2 (continued).

tance was significantly reduced compared to unmodified sodium channels (Cachelin et al. [9]) and also when compared with conductances of sodium channels affected by other modifiers, i.e., ATX-II (Schreibmayer et al. [16]), Chloramine-T (Nagy [15]) and S-DPI (Kohlhardt et al. [19]). This finding is in agreement with reports by Sigel [20,21] and Yoshii and Narahashi [13].

Original records are shown in Fig. 3a. Only one conductance level is observed with a slope conductance (see Fig. 3b) of 5.0 ± 0.3 pS therefore assigned as g^{v}_{cll}. This value is intriguingly close to the value found for state II of S-DPI/veratridine modified channels, i.e. g^{a+v}_{cll}: 4.7 ± 0.6 pS.

In light of the six sublevels observed with the S-DPI/veratridine mixture, it was of interest to investigate the effect of S-DPI alone.

S-DPI modified sodium channels (index s)

In two different cell attached membrane patches effects of 200 μM S-DPI on sodium channels were investigated. Under these conditions sodium channel openings could be induced by hyper- and de-polarization of the membrane patch (Fig. 4a). One current level was predominant. The slope conductance of this current level was determined to be 13.7 ± 0.7 pS (Fig. 4b). However, among the 132 individual records examined, 5 sublevel fluctuations (in 3.8% of all traces) could be detected and assigned as I^{s}_{cll}. They had a current ratio of 0.31–0.41 compared to the main level, i.e., I^{s}_{cVI}.

One further sublevel (at a frequency of 3.8%) was detected (see Fig. 4c B). The fractional current of this sublevel current compared to the main current level (I^{s}_{cVI}) was 0.61–0.74.

Sodium channels modified by a mixture of ATX-II and veratridine (index a + v)

The effects of ATX-II alone on the cardiac sodium channel have been covered extensively by preceding papers (Schreibmayer et al. [22,16]). Slope conductance of the ATX-II modified channel had been estimated to be 11.5 pS in these earlier studies. It agrees fairly well with the value of 10.8 pS reported by Nagy [15] for neuroblastoma cells at about 10 °C.

In view of the six sublevels observed with the veratridine/S-DPI mixture, we also investigated the effects of veratridine in combination with ATX-II, to see whether the observed sublevels are characteristic for a specific modifier mixture or intrinsic properties of the channel.

Four different cell-attached membrane patches were formed with 500 nM ATX-II plus 20 μM veratridine in standard pipette solution.

Sodium channel openings were easy to observe at steady-state conditions (constant pipette potential); see Fig. 5a.

Whereas level II for veratridine alone was observed only after depolarizing voltage jumps and disappeared almost completely after prolonged depolarization (see Fig. 3c) level II was observed frequently at maintained depolarization when both veratridine and ATX-II were present. Neither under the action of ATX-II (Schreibmayer et al. [16]) nor veratridine alone (this study) could such a gating behaviour of the channel be observed. This observation clearly indicates, that openings of the channel by ATX-II are required to give veratridine access to the channel under steady-state conditions. Indeed, sublevel fluctuations to the g^{a+v}_{cll} level are often preceeded by full openings of the channel (see arrows in Fig. 5a B). This is the first direct evidence derived with the patch-clamp method for the positive allosteric interaction of receptor domain II and III of the sodium channel, which has been postulated based on radioligand binding studies (Catterall and Coppersmith [23]).

Two mainly populated sublevels were observed, g^{a+v}_{cll} and g^{a+v}_{cV} with slope conductances of 4.6 ± 0.4 pS and

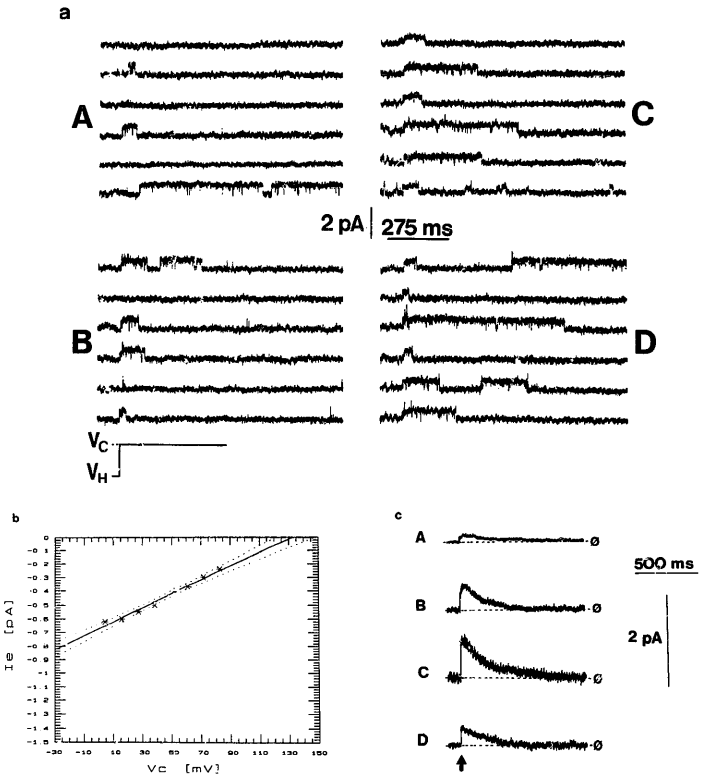

Fig. 3. Sodium currents through sodium channels modified by veratridine only (100 μM). (a). The traces were obtained by repetitive hyper- and de-polarization of the patch as in Fig. 1a. V_H and V_C values were: A: +40 mV, −16 mV; B: +40 mV, −27 mV; C: +40 mV, −38 mV; D: +40 mV, −61 mV. Sampling rate was 3 kHz and LP = 1 kHz. (b). Current-voltage relationship of the only level observed. Slope conductance: g_{ell}^{*} was 5.0±0.27 pS, correlation coefficient: 0.99. (c). Averaged single-channel currents to demonstrate practically complete inactivation of veratridine modified sodium channels after voltage jumps. A–D correspond to Fig. 3a A–D. Number of individual records averaged: A: 105, B: 107, C: 72, D: 68.

11.8 ± 2.9 pS, respectively (see Fig. 5b). The larger error of the latter value is due to the short residency time of the channel in this state.

Current levels I, III, and IV were observed also, as exemplified in Fig. 5c. Relative occurrences of these sublevels were: 29 observations of level I (in 3.2% of the

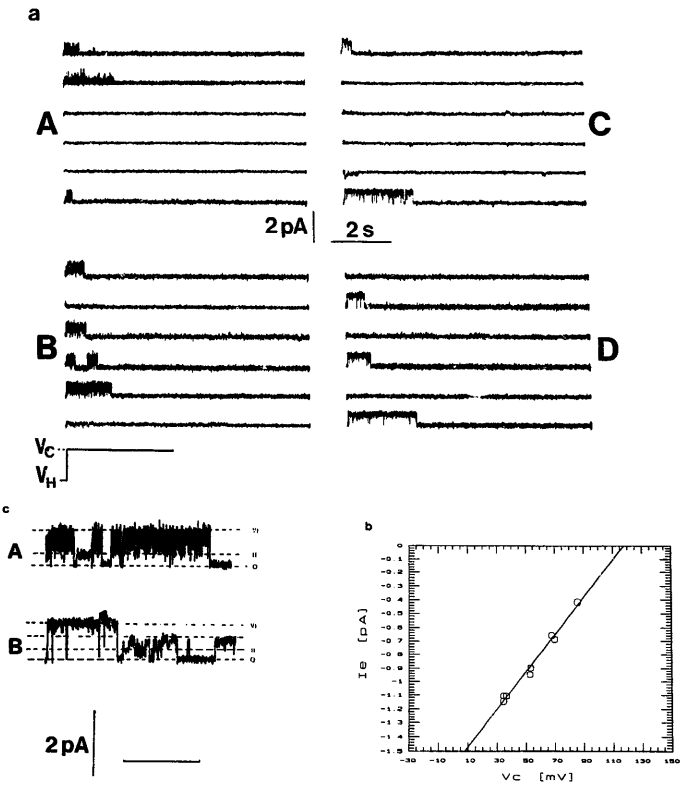

Fig. 4. Sodium currents through sodium channels modified by S-DPI (200 μM). (a). Sodium channel currents were elicited by repetitive hyper- and de-polarization of the patch as in Fig. 1a. V_H and V_C values were: A: +41 mV, −9 mV; B: +41 mV, −18 mV; C: +41 mV, −27 mV; D: +23 mV, −35 mV. Sampling rate was 1 kHz and LP was 250 Hz. (b). I^{ss}_{eVI} vs. V_C. Current-voltage relationship of the main level VI. Slope conductance g^{ss}_{eVI} was 13.7±0.7 pS, correlation coefficient: 0.99. (c). Selected current events showing sublevels II and IV. V_C, LP and Δt values were: A: −37 mV, 100 Hz, 3.2 s; B: −35 mV, 100 Hz, 2.2 s.

909 records evaluated), 7 of level III (0.8%) and 28 of level IV (3.1%). In the absence of I^{a+v}_{eVI} events we have normalized the currents of these levels to 3-times I^{a+v}_{eII}. The resulting current ratios were as follows: 0.13–0.19, 0.51–0.62, 0.71–0.81 and 0.84–0.94 for I^{a+v}_{eI}, I^{a+v}_{eIII}, I^{a+v}_{eIV} and I^{a+v}_{eV}, respectively.

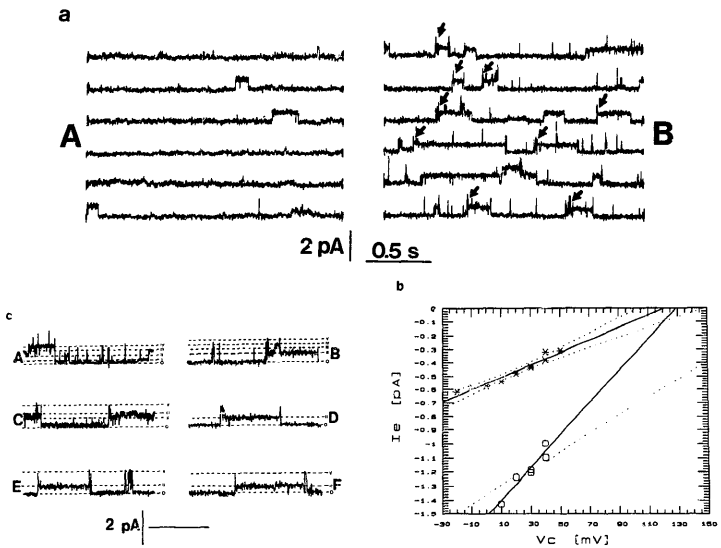

Fig. 5. Sodium currents through cardiac sodium channels modified by veratridine (100 μM) and ATX II (50 nM). (a). Original records obtained under steady-state (constant pipette voltage (V_C) conditions. A: $V_C = +10$ mV; B: $V_C = -40$ mV. Sampling frequency was 5 kHz and LP was 500 Hz (b). I_{ss}^{a+v} vs. V_C. Current-voltage relationships of sublevels II (•) and V (○). Slope conductances were $g_{aII}^{a+v} = 4.6 \pm 0.4$ pS, correlation coefficient: 0.97; $g_{aV}^{a+v} = 11.8 \pm 1.9$ pS, correlation coefficient: 0.95. (c). Selected current records showing sublevels II, III, IV and V. V_C, LP and Δt-values were: A: -20 mV, 250 Hz, 0.744 s; B: -20 mV, 500 Hz, 0.24 s; C: -20 mV, 500 Hz, 0.51 s; D: -30 mV, 500 Hz, 0.16 s; E: -30 mV, 500 Hz, 0.24 s; F: -40 mV, 500 Hz, 0.2 s.

TABLE I

Reversal potentials of substate currents

cr (current ratio): corresponding substate has been detected, but relative frequency of occurrence and/or distribution at different voltages was too low for meaningful statistical analysis. Current ratio, however, could be calculated (see Table III). –: corresponding substate not observed under the given experimental conditions.

Modifier used	Concn. Na^+ (mM)	Reversal potential of state n (mV)					
		n = I	n = II	n = III	n = IV	n = V	n = VI
s + v	71.5	cr	104.0 ± 28.2	–	–	–	95.2 ± 28.0
	303.0	cr	103.5 ± 12.2	cr	110.0 ± 13.9	cr	108.5 ± 17.3
	140.0	cr	106.5 ± 21.2	cr	cr	cr	112.9 ± 13.9
v	140.0	cr	131.2 ± 13.2 *	–	–	–	–
s	140.0	–	cr	–	cr	–	116.9 ± 9.3
a + v	140.0	cr	114.5 ± 27.8	cr	cr	119.6 ± 36.0	–

* U_{revII}^{v} differs significantly from U_{revII}^{a+v} ($\alpha < 0.05$).

Comparison of observed substates

Selectivity for sodium. Reversal potentials of sodium currents were estimated by extrapolation from the linear regression fits of I_c vs. V_c shown in figs. 1b, 2b, 2e, 3b, 4b and 5b. Estimated reversal potentials ± standard deviations (S.D.) are listed in Table I.

Comparison of different modifiers. At 140 mM sodium reversal potentials for state II could be measured for three different modifying conditions: s + v, v and a + v. The null-hypothesis H_0: $U^x_{rev} = U^y_{rev}$ was tested according to Student's *t*-test (Kreyszig [24]). No statistically significant difference was found between U^{s+v}_{revII} and U^{a+v}_{revII} as well as between U^{a+v}_{revII} and U^{v}_{revII}. The difference between U^{s+v}_{revII} and U^{v}_{revII}, however, was significant with an error probability of $\alpha < 0.05$. Two reversal potentials (U^{s+v}_{revVI} and U^{s}_{revVI}) could be obtained for state VI. These values did not differ significantly. Although the permeability ratio P_{Na^+}/P_x (x: intracellular ions) seems to be altered under the action of veratridine alone, Na^+ is the main permeating ion for state II as well as for state VI for all modifiers (and their combinations) tested.

Comparison of different sublevels. At 303 mM U^{s+v}_{rev} values could be obtained for states II, IV and VI. There was no significant difference between these three values as estimated by Student's *t*-test. Therefore, sodium selectivity remains constant for states II, IV and VI. U^{s+v}_{rev} values for states II and VI were also the same at 71.5 mM as well as at 140 mM sodium. U^{a+v}_{rev} values could be measured for states II and V, respectively, and were identical as well. These data clearly demonstrate conserved ion selectivity at least for states II, IV, V and VI.

Comparison of slope-conductances. The slope conductances estimated under the different experimental conditions are listed in Table II.

140 mM sodium: Individual slope conductances for state II, obtained under s + v, v and a + v, were compared by means of Student's *t*-test. The null-hypothesis

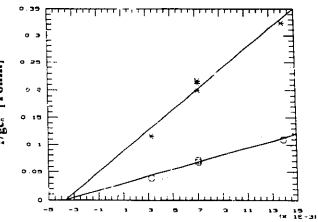

Fig. 6. Dependences of substate conductances g_{eII} (•) and g_{eVI} (○) on sodium ion concentration. The data are plotted in a Lineweaver-Burk diagram. $K_{Na^+,II}$ was calculated by linear regression to be 303 mM and $g_{eII_{max}}$ 14.6 pS; $K_{Na^+,VI}$ was 286 mM and $g_{eVI_{max}}$ 42.8 pS. The data for sublevel II include values of g^x_{eII} and g^{s+v}_{eII} at 140 mM sodium chloride in addition to g^{s+v}_{eII} at 71.5, 140 and 303 mM sodium chloride. The data for sublevel VI include values of g^s_{eVI} at 140 mM sodium chloride in addition to g^{s+v}_{eVI} for 71.5, 140 and 303 mM sodium chloride.

H_0: $g^x_{e_n} = g^y_{e_n}$ could not be rejected, which is equivalent to the notion that there is no significant difference between conductances of state II for these modifiers. This applies also to the g_{eVI} values for s and s + v and to the g_{eV} values for a + v and a (for the latter value see Schreibmayer et al. [16]). These findings and the equal distribution of current ratios (see below) justify *a posteriori* the consecutive numbering of substates from I to VI for all the different experimental conditions (sodium and modifier variation).

Variation of sodium ion concentration. Sodium binding to the channel was investigated in order to test whether the affinity of the channel for sodium in different substates might be different. The data in Table II

TABLE II

Slope conductances of substates

cr and –: see legend to Table I.

Modifier used	Concn. Na^+ (mM)	Conductance of state *n* (pS)					
		n = I	*n* = II	*n* = III	*n* = IV	*n* = V	*n* = VI
s+v	71.5	cr	3.1±0.9	–	–	–	9.0±1.8
	303.0	cr	8.7±0.3	cr	16.2±1.2	cr	24.5±1.7
	140.0	cr	4.7±0.6	cr	cr	cr	14.2±0.8
v	140.0	–	5.0±0.3	–	–	–	–
s	140.0	–	cr	–	cr	–	13.7±0.7
a+v	140.0	cr	4.6±0.4	cr	cr	11.8±2.9	–
a	140.0	–	–	–	–	11.5±1.0 [a]	–

[a] Taken from Schreibmayer et al. [16].

TABLE III

Ranges of current ratios (cr) of substates

Current level ranges or individual substate currents are expressed as fractions of the current level marked with an * (mostly level VI). –: see legend to Table I.

Modifier used	Concn. Na^+ (mM)	Current ratios of state n					
		n = I	n = II	n = III	n = IV	n = V	n = VI
s + v	71.5	0.18–0.28	0.34–0.44	–	–	–	1.00 *
	303.0	0.16–0.22	0.27–0.35	0.38–0.56	0.64–0.70	0.78–0.88	1.00 *
	140.0	0.17–0.23	0.23–0.33	0.46–0.54	0.62–0.72	0.76–0.90	1.00 *
v	140.0	–	0.34–0.38 [a]	–	–	–	–
s	140.0	–	0.31–0.41	–	0.61–0.74	–	1.00 *
a + v	140.0	0.13–0.19 [b]	0.33 *	0.51–0.62 [b]	0.71–0.81 [b]	0.84–0.94 [b]	–
	$cr_{(n)}$ [c]	0.20	0.34	0.51	0.69	0.85	1.00 *
	$cr_{(n)} \times 6$	1.2	2.0	3.1	4.1	5.1	6.0 *

[a] In the absence of any current level corresponding to level VI, this current ratio range was calculated by comparing slope conductances.
[b] In the absence of level VI, current levels were normalized to $3 \cdot I_{elI}^{s+v}$ (cr_{II}^{s+v} is marked with * for that reason).
[c] $cr_{(n)}$ represent average values of cr values listed.

were evaluated according to the Michaelis-Menten equation:

$$g_e([Na^+]) = g_{e_{max}} \cdot 1/(1 + K_{Na^+}/[Na^+]) \quad (1)$$

g_e values for states II and VI were plotted in a Lineweaver-Burk diagram for 71.5, 140 and 303 mM Na^+, respectively (see Fig. 6). Data for s, v, s + v and a + v were pooled. $g_{e_{maxII}}$ was calculated to be 14.6 pS by linear regression and $g_{e_{maxVI}}$ was 42.8 pS (note that the ratio $g_{e_{maxVI}}/g_{e_{maxII}}$ is 2.9). The null-hypothesis H_0: $1/g_{e_{maxII}} = 1/g_{e_{maxVI}}$ was tested by means of a small sample t-test (Kleinbaum and Kupper [25]) and was rejected with $\alpha < 0.05$. The corresponding K_{Na^+} values were estimated to be 303 and 286 mM sodium for states II and VI, which agrees fairly well with the data given by Hille [26]. H_0: $K_{Na^+II} = K_{Na^+VI}$ was tested and could not be rejected ($\alpha > 0.4$). These findings indicate that the affinity for sodium ions is maintained during substate behaviour.

Due to the relative low conductances and fast gating we have not been able to study ion fluxes at Na^+ concentrations below 71.5 mM. Therefore we might have missed high affinity binding sites of the channel for sodium ions. Although in the literature no evidence exists for them, such binding sites have been reported for a Ca^{2+}-activated K^+ channel (Vergara et al. [27]). Other ions than Na^+ present in the intra- and extracellular milieu's might lead to altered Michaelis-Menten behaviour if they compete with Na^+-binding sites or alter them allosterically [27]. A block of the cardiac sodium channel by Ca^{2+} ions, for instance, has been studied extensively by Nilius [28].

All these possible effects of parameters on our saturation experiments, however, have been virtually the same on substates II and VI.

Sublevel currents. The estimated ranges of current ratios (cr), i.e. cr – S.D. to cr + S.D., of the observed sublevels for all types of modification and variation of sodium concentration are listed in Table III. Inspecting the data, it becomes apparent that current ratios are almost identical for a given substate regardless of Na^+ concentration (71.5, 140 or 303 mM) or modifier used (s, v, s + v or a + v). Therefore, mean values for the current ratios of all six observed channel open states were calculated (Table III lower part). These current ratios were multiplied by the number of observed open states, i.e., six. The results lead us to the assumption that all observed current ratios are multiples of the smallest current ratio observed, of state I.

Discussion

This study presents data on subconductance states of the sodium channel elicited by three inactivation-modifying agents, veratridine, S-DPI, and ATX-II, applied either singly or in combination. The observed effects of these agents can be compared directly as the different modifications were applied under identical experimental conditions, i.e., (i) to the same sodium channel subtype (cardiac from adult rats) in (ii) cell attached membrane patches using (iii) a pipette solution mimicking extracellular electrolyte conditions. For the three agents both the conductance of the predominant level and the number of observable levels in isolated current events were different. Furthermore, modifier pairs elicited more resolvable subconductance states than their individual application did. However, summarizing these observations (listed in Table III) led to the most remarkable finding that all conductance levels fitted a pattern of six levels with approximately even spacings. Apparently,

the modifiers do not have unique effects on channel conductance; instead, they induce different populations among six possible conductance states. Veratridine locks the channel in state II and S-DPI primarily in state VI with occasional sojourns to level IV or II. In contrast, the ligand pairs S-DPI/veratridine and veratridine/ATX elicit additional levels, not of some arbitrary value but of just those values which complement the levels for single modifiers to a complete set of six equidistant levels. From this we conclude that these six equidistant conductance states are genuine to the sodium channel as possible states.

Existence of substates of the unmodified Na^+ channel had been postulated already in 1983 (Nagy et al. [29]) on the basis of at least three Gaussian components required to fit amplitude histograms. It was only recently, while preparing this manuscript, that the first direct observation of substates of unmodified channels was reported (Patlak [11]). Besides other less resolved and less populated substates there was one most common level at 35%of the normal current which corresponds to level II in our nomenclature with state VI as normal state. Moreover, the same study showed a sublevel after removal of inactivation by S-DPI at again 35% of the normal level in agreement with our data. – The main current level of BTX-treated channels is consistent with level IV since its current was observed to be twice as large as that observed for veratridine (Garber and Miller [30]). BTX-modified channels showed, in addition, subconductance levels of 25% and a flickering level at about 50% (Green et al. [31]) of the main level, which are values expected for levels I and II, respectively. Similar observations were made by Urban et al. [32]. – The extensive study of Nagy [15,33] on sublevels in Na^+ channels of neuroblastoma cells treated with chloramine-T, sea anemone toxin, and scorpion toxin yielded a consistent set of sublevels for the three agents at 25, 53, and 128% of the main level with standard deviations of typically 5%. These data would formally match our set of six values if the main current level represents level IV. This assignment finds support in the observation of definitely larger currents than the main currents (100% levels). In this respect it is of interest that in the same type of cells (neuroblastoma) a Na^+-channel substate of 66% of the main level was observed when deltamethrin was used to slow down inactivation (Chinn and Narahashi [14]). The current of the main level was similar to that of the native channel so that the 66% substate matches our sublevel IV.

Therefore, the available data in the literature on Na^+-channel substates are at least not inconsistent with our finding of six evenly-spaced conductance states of the sodium channel, where state VI corresponds to the mainly observed state of the native channel.

The sodium channel is actually not the first channel for which a *regular* substate pattern has been evidenced. There is an extensive list of cation and chloride channels including channels activated by voltage and by ligands (glutamate, GABA, glycine, acetylcholine) which show *regular* substate patterns. The literature on this has been reviewed up to 1986 by Fox [8]. Most common numbers of conductance states occurring as integer multiples of a smallest conductance are 3, 4 and 6. The largest number of 16 equally-spaced subconductance levels with the same ion selectivity has been found for voltage-dependent K^+ channels (Kazachenko and Geletyuk [34] and Schindler and Schreibmayer [35]) and a Cl^- channel (Geletyuk and Kazachenko [36]). The property of evenly spaced substate patterns extents as well to Ca^{2+} channels as recently shown (Hymel et al. [37,38]).

What could be the physical basis of such a regular substate pattern? Two possible causes for substates can be excluded directly from our data as outline in the last section in Results. Reversal potentials of different substates were sufficiently identical to conclude that substates are not caused by discrete changes of the selectivity for sodium against the internal ion composition. Neither do they appear to be caused by discrete changes of Na^+ binding to saturable sites of the channel since the concentrations at halfsaturation for sublevels II and VI were very similar.

Therefore, the observed sublevel pattern should be caused by discrete changes of the translocation rate (k_t) of sodium ions at constant sodium selectivity and binding, where k_t assumes approximately integer multiples of a smallest value; i.e. $k_{t,n} = k_{t,1} \cdot n$ with $n = 1$ to 6. In the following we try to analyze the consequences of this rather severe constraint on existing models for sodium channel conduction.

All current models of sodium channels assume that each single-current event observed in patch clamp studies arises from sodium flux through a single pathway. Each ion transversing this pathway experiences a 'free energy profile', which is a reflection of the pathway's structure. This profile is commonly modeled by a series of energy minima representing ion residency sites which are separated by activation energy barriers. Ion hopping rates from site to site are then related to barrier heights (free energy of activation, $\Delta G^{\ddagger}$) on the basis of absolute rate theory (Glasstone et al. [39]). This yields expressions for the net ion flux in response to an electrical potential gradient when combined with standard chemical kinetics (Woodbury [40]). The most fully developed model of the Na^+ channel (Hille [41]) shows four barriers and three sites which are assumed to be occupied by no more than one ion at any time (one ion pore). Approaching from the outside, there is first a low barrier and then a well. Depth and location of this well are constrained by the experimentally determined K_{Na^+} for sodium ions, which was evidenced here not to change significantly during transitions between sub-

states. Then there is a high barrier (B2), the 'rate-limiting selectivity filter', followed by further lower barriers which were introduced to adjust predicted current-voltage relationships of the open channel to the experimental one. The height of B2 for permeating Na^+, i.e. $\Delta G^{\ddagger}_{Na}$, was adjusted to the observed single channel conductance with physiological Na^+ concentrations. Permeability ratios for other ions (P_{Na^+}/P_x) were accounted for by corresponding increases, i.e. $\delta[\Delta G^{\ddagger}_x]$, of the height of B2 sensed by these ions, i.e. $\Delta G^{\ddagger}_x$, which reads in first approximation *:

$$\delta[\Delta G^{\ddagger}_x] = \Delta G^{\ddagger}_x - \Delta G^{\ddagger}_{Na} = RT \cdot \ln(P_{Na^+}/P_x) \qquad (2)$$

This yields increases of about $0.1 \cdot RT$ and $2.7 \cdot RT$ for Li^+ and K^+ ions, respectively.

Within this model, the observed substate fluctuations must be accounted for by discrete fluctuations of the height of the rate-limiting barrier B2. The current ratios of the sublevels $cr(n) \approx n/6$ with $n = 1$ to 6 correspond to barrier height increases $\delta[\Delta G^{\ddagger}_{Na}(n)]$ above its normal height of *:

$$\delta[\Delta G^{\ddagger}_{Na}(n)] = RT \cdot \ln(6/n) \qquad (3)$$

or

$$\Delta G^{\ddagger}_{Na}(n) = \Delta G^{\ddagger}_{Na}(6) + RT \cdot \ln 6/n$$

These logarithmic energy increments are of similar magnitudes ($0.2 \cdot RT$ for state V and $1.8 \cdot RT$ for state I) when compared with the selectivity corrections $\delta[\Delta G^{\ddagger}_x]$.

The observed conservation of ion selectivity during substate transitions requires that the barrier height changes for Na^+ ions are strictly coupled to those of other ions (predominantly K^+ ions in our cell-attached experiments). Insertion of Eqn. 3 into Eqn. 2 yields for substate independent permeability ratios:

$$\Delta G^{\ddagger}_x(n) = \Delta G^{\ddagger}_{Na}(n) + RT \cdot \ln(P_{Na^+}/P_x); \quad n = 1 \text{ to } 6$$

$$= \Delta G^{\ddagger}_{Na}(6) + RT \cdot \ln(P_{Na^+}/P_x) + RT \cdot \ln(6/n) \qquad (4)$$

Eqns. 3 and 4 represent a set of six logarithmically spaced transition state energies for Na^+ permeation which, for other ions than Na^+, remains the same but raised by constant selectivity corrections. We are not aware of any physical explanation which may account for such a pattern of energies of the main barrier. The inherent difficulties may be exemplified by the following argumentation. Among the different possible contributions to $\Delta G^{\ddagger}(n)$ the first choice candidate for causing substates by discrete changes is the electrostatic component of the energy barrier. The physical cause, which may relate to changes of charge, charge interactions, and conformational changes, may generate the $\Delta G^{\ddagger}(n)$ patterns of Eqns. 3 and 4 provided that it: (i) alters the electrostatic component of the energy barrier for different ions including Na^+ and K^+ by the same amounts, (ii) generates the very particular set of six logarithmically spaced barrier height increases, (iii) does not affect those contributions to the energy barrier which generate selectivity, that is, contributions of ions size, mass, or, more generally, of the delicate balance between hydration- and site-interaction energies (Eisenmann [42]) and (iv) does not affect the primary energy well providing the saturable site for sodium binding. While (i) may be readily accepted, it is condition (ii) by itself but even more in combination with (iii) and (iv) which appears extremely difficult, if not impossible, to realize by alterations of the structure and ionic interactions at the position of the rate-limiting and selectivity generating structure in the narrow part of the pore (see for instance the molecular model proposed by Hille [41,26]).

If there were only one substate of arbitrary current fraction instead of six regulary spaced levels, a molecular interpretation would appear still feasible to us even at conserved ion selectivity and ion binding. Indeed, a recent report on the DHP-receptor Ca^{2+}-channel proposed that the occurrence of a particular substate (observed only in the presence of monovalent ions as permeant ions) relates to the protonation of an external group which triggers a conformational change to a state with lower conductance with little change of selectivity (Pietrobon et al. [43]).

The above treatment certainly does not qualify to reject the one pore assumption for the sodium channel since it has been based on a rather simplistic model compared to the reality. It was meant to indicate conceptual problems raised by the data. It remains to be seen whether other or more realistic models offer explanations for observing such regular substate pattern, including that the Na^+ channel may represent a multi-ion pore, as the results of Begenesish and Cahalan [44] suggest for the sodium channel from squid, or considering more than one binding site for Na^+ ions. More generally, many channels including the Na^+ channel have funnel-shaped vestibules providing a conditioned environment for the selective narrow region deeper in the pore. This, suggests a progressive shift from a bulk solution like to a selectivity filter situation. Several effects of the vestibule on channel conductance have been proposed by Dani [45] by coupling a two Eyring-barrier model to continuum modeled vestibules of defined size, shape, and surface charge. In other attempts, shape has been introduced into rate-theory barriers

* For the sake of a more transparent argumentation only, we equate the net translocation rate with the jump rate from the external primary energy well over the 'rate-limiting selectivity barrier B2'. Complete calculations yield only slight corrections to the given barrier height changes ($\delta[\Delta G^{\ddagger}_x]$) which are of no relevance for the conclusions drawn.

(Eisenmann et al. [46]). Effects of molecular motion on channel conductance has been modeled via time-dependent fluctuations in the free energy profile (Frehland [47], Läuger et al. [48]) and by molecular dynamics simulations (Fischer et al. [49], Mackay et al. [50]). Coupling vestibules or introducing shape to Eyring-barrier models has brought considerable insight but not of the kind which would help to interpret multiple substate events by one-pore models, at least at the present level of understanding. Certainly, treatment of both realistic structures and dynamics in model calculations, a level which is not yet been attained, may open new possibilities to explain multiple conductance states in single channels, possibly as normal modes of dynamic interactions between channel structure and passing ions.

Finally, it should be added, that any attempt to explain regular substate patterns should take into account that such patterns are found for many different types of channels. This suggests a common mechanism which, therefore, should be independent of the particular structural features of each channel.

In view of these difficulties to rationalize multiple-state sodium current events by transitions in one pore ('monopore' concept) one may alternately consider that they reflect the concerted activity of associated pores ('oligopore' concept). This concept dates back to 1978 when porin channels had been observed to gate cooperatively in porin associates (Schindler and Rosenbusch [5,6]) and has since been shown to apply to several other channel proteins using a particularly designed reconstitution strategy (for a review of strategy and results see Schindler [51]). The same properties which render the 'monopore' picture difficult to accept are directly expected when the sodium channel is visualized as an 'oligopore'. Strictly coupled gating of six parallel pathways in a sodium channel protein oligomer would yield apparent two state transitions between zero conductance and the combined conductance of the six pathways ('protopores'), which would then correspond to the normally observed sodium channel conductance. Occasional less strict coupling or modifier induced perturbation of the all-or-none cooperativity between 'protopores' would result in current events showing substates with the following expected properties (i) six evenly spaced conductance levels * where (ii) all levels show the same selectivity for Na^+ ions and (iii) the same Na^+ saturation characteristics. The experimental data reported here match these predicted properties in all parts. We are not aware of any literature data on the sodium channel which would be in contradiction to the proposal that sodium channel events originate from 'oligopores'. The existing Eyring-barrier models for the Na^+ channel can, for example, be adapted to the 'oligopore' situation without inflicting any of the reported conclusions. The reference height of the main energy barrier, which is a free parameter and commonly adjusted to the normal channel conductance, may as well be adjusted to the conductance of the 'protopore' (substate I) by adding about 1.8 *RT*. In our data and in the literature on substates levels II, IV and VI occur more frequently and/or more stabilized than the uneven multiples of level I. This is actually expected from theories of allosteric interactions in associates with even numbers of protomers, such as six 'protopores'. However, the above discussion left as remote possibility that the elementary pore may have one substate at half conductance. In this case, the observed substate pattern would reflect concerted activities of three 'protopores' each with level II as main conductance and level I as subconductance. The higher occurrence of even multiples may then reflect that concerted gating is more likely for fully open 'protopores' than for 'protopores' in substates. In this respect it may be of interest, that the charge movement during Na^+-channel gating was recently found to occur in about three steps or packets of about 1/3 of the whole gating charge [52].

We conclude that the 'oligopore' concept provides at present the only direct explanation for sodium channel current events. In addition, it is sufficiently general, i.e., not dependent on particular structural aspects, to account for level multiplicity at constant selectivity as a widespread phenomenon among channels (Fox [8]). It would be too premature to speculate about possible mechanisms of 'protochannel' coupling. At present it appears warranted to apply assays which may allow for clear decisions in this conceptual dilemma whether 'oligopores' or 'monopores' are the underlying structure of the observable multistate current events commonly termed 'single-channel events'. This obviously requires directly relate protein organization and electrical activity and may therefore not be expected from patch clamp studies. More specifically, it requires at least direct knowledge of the number of channel proteins in the molecular unit for which channel activity is observed. This has been approached for several channel proteins by a particular designed reconstitution strategy (Schindler [51]) which led to the identification of at least four 'oligopores' (Schindler and Rosenbusch [6], Schindler et al. [53], Hymel et al. [37,38]). From our current application of this strategy to the sodium channel we expect a clear decision whether the sodium channel is also an 'oligopore' as it appears likely to us on the basis of the above discussion. If so, this would

* Flux coupling between pores in "oligopores" may induce slight deviations from evenly spaced conductance states as it has been shown for porin "triple-pores" (Engel et al. [55]).

bear rather dramatic consequences on the understanding of excitation and on ligand effects *.

Acknowledgements

We thank Prof. G. Scholtysik (Sandoz AG, Basel) for his gift of S-DPI 201-106 to our 'Schwerpunktsprogramm S 45', Prof. H. Glossmann (Institute for Biochemical Pharmacology, Innsbruck) for distributing the substance to us and Prof. K. Pfeiffer (Institute for Physiology, Graz) for valuable discussions about statistical analysis of the data. The assistance of B. Spreitzer and S. Bauer in preparing myocytes and typewriting of the manuscript, and the computational work on statistics by Dr. M. Windisch (Institute for Zoology, Graz) are greatly acknowledged. We also wish to thank Dr. L. Hymel and L. Patassy for critical reading of the manuscript. This work was supported by the Austrian Research Fund (S 45).

References

1 Neher, E. and Sakmann, B. (1976) Nature 260, 799–802.
2 Horn, R. and Patlak, J. (1980) Proc. Natl. Acad. Sci. 77, 6930–6934.
3 Sigworth, F.J. and Neher, E. (1980) Nature 287, 447–449.
4 Horn, R., Patlak, J. and Stevens, C.F. (1981) Biophys. J. 36, 321–327.
5 Schindler, H. and Rosenbusch, J.P. (1978) Proc. Natl. Acad. Sci. USA 75, 3751–3755.
6 Schindler, H. and Rosenbusch, J.P. (1981) Proc. Natl. Acad. Sci. USA 78, 2302–2306.
7 Latorre, R. and Alvarez, O. (1981) Physiol. Rev. 61, 77–150.
8 Fox, J.A. (1987) J. Membr. Biol. 97, 1–8.
9 Cachelin, A.B., de Peyer, J.E., Kokobun, S. and Reuter, H. (1983) J. Physiol. 340, 389–401.
10 Kunze, D.L., Lacerda, A.E., Wilson, D.L. and Brown, A.M. (1985) J. Gen. Physiol. 86, 691–719.
11 Patlak, J.B. (1988) J. Gen. Physiol. 92, 413–430.
12 Quandt, F.N. and Narahashi, T. (1982) Proc. Natl. Acad. Sci. USA 79, 6732–6736.
13 Yoshii, M. and Narahashi, T. (1984) Biophys. J. 45, 184a.
14 Chinn, K. and Narahashi, T. (1986) J. Physiol. 380, 191–207.
15 Nagy, K. (1987) Eur. Biophys. J. 15, 129–132.
16 Schreibmayer, W., Kazerani, H. and Tritthart, H.A. (1987) Biochim. Biophys. Acta 901, 273–282.
17 Hamill, O.P., Marty, A., Neher, E., Sakmann, B. and Sigworth, F.J. (1981) Pfluegers Arch. 391, 85–100.
18 Bezanilla, F. (1985) Biophys. J. 47, 437–441.
19 Kohlhardt, M., Froebe, U. and Herzig, J.W. (1986) J. Membr. Biol. 89, 163–172.
20 Sigel, E. (1987) J. Physiol. 386, 73–90.
21 Sigel, E. (1987) Pfluegers Arch. 410, 112–120.
22 Schreibmayer, W., Kazerani, H. and Tritthart, H.A. (1986) Arch. Pharmacol. 334, R11/45.
23 Catterall, W.A. and Coppersmith, J. (1981) Mol. Pharmacol. 20, 533–542.
24 Kreyszig, E. (1975) Statistische Methoden und ihre Anwendungen, pp. 218–221, Vandenhoeck and Ruprecht, Göttingen.
25 Kleinbaum, D.G. and Kupper, L.L. (1978) Applied Regression Analysis and other Multivariable Methods, pp. 100–103, Duxbury Press, North Scituate, MA.
26 Hille, B. (1984) Ionic Channels in Excitable Membranes, pp. 601–617, Sinauer Associates Inc., Suderland, MA.
27 Vergara, C., Moczydlowski, E. and Latorre, R. (1984) Biophys. J. 45, 73–76.
28 Nilius, B. (1988) J. Physiol. 399, 537–558.
29 Nagy, K., Kiss, T. and Hof, D. (1983) Pfluegers Arch. 399, 302–308.
30 Garber, S.S. and Miller, C. (1987) J. Gen. Physiol. 89, 459–489.
31 Green, W.N., Weiss, L.B. and Anderson, O.S. (1987) J. Gen. Physiol. 89, 841–872.
32 Urban, B.W., Recio-Pinto, D.S. and Parnicas, M. (1987) Pfluegers Arch. 408, R31?.
33 Nagy, K. (1988) J. Membr. Biol. 106, 29–40.
34 Kazachenko, V.N. and Geltuyk, V.J. (1984) Biochim. Biophys. Acta 773, 132–142.
35 Schindler, H. and Schreibmayer, W. (1985) in Molecular Basis of Nerve Activity (Changeux, J.-P., Hucho, F., Maelicke, A. and Neumann, E., eds.) pp. 285–297, de Gruyter, Berlin and New York.
36 Geletyuk, V.J. and Kazachenko, V.N. (1985) J. Membr. Biol. 86, 9–15.
37 Hymel, L., Inui, M., Fleischer, S. and Schindler, H. (1988) Proc. Natl. Acad. Sci. USA 85, 441–445.
38 Hymel, L., Striessnig, J., Glossmann, H. and Schindler, H. (1988) Proc. Natl. Acad. Sci. USA 85, 4290–4294.
39 Glasstone, S., Laidler, K.J. and Eyring, H. (1941) The Theory of Rate Processes, Mc Graw-Hill, New York.
40 Woodbury, J.W. (1971) in Chemical Dynamics, Papers in Honor of Henry Eyring (Hirschfelder, J.O., ed.), pp. 601–617. John Wiley, New York.
41 Hille, B. (1975) J. Gen. Physiol. 66, 535–560.
42 Eisenmann, G. and Horn, R. (1983) J. Membr. Biol. 76, 197–225.
43 Pietrobon, D., Prod'hom, B. and Hess, P. (1988) Nature 333, 373–376.
44 Begenesich, T.B. and Cahalan, M.D. (1980) J. Physiol. 307, 217–242.
45 Dani, J.A. (1986) Biophys. J. 49, 607–618.
46 Eisenmann, G., Dani, J.A. and Sandblom, J. (1985) Recent Advances in the Theory and Application of Ion Selective Electrodes in Physiology and Medicine (Kessler, M., Harrison, D.K. and Hoper, J., eds.), Springer Verlag, Berlin.
47 Frehland, E. (1979) Biophys. Struct. Mech. 5, 91–106.
48 Läuger, P., Stephan, W. and Frehland, E. (1980) Biochim. Biophys. Acta 602, 167–180.
49 Fischer, W., Brickmann, J. and Läuger, P. (1981) Biophys. Chem. 13, 105–116.
50 Mackay, D.H.J., Berens, P.H., Wilson, K.R. and Hagler, A.T. (1984) Biophys. J. 46, 229–248.
51 Schindler, H. (1989) Meth. Enzym. 171, 225–253.
52 Conti, F. and Stühmer, W. (1989) Eur. Biophys. J. 17, 53–59.
53 Schindler, H., Spillecke, F. and Neumann, E. (1984) Proc. Natl. Acad. Sci. USA 81, 6222–6226.
54 Nilius, B., Vereecke, J. and Carmeliet, E. (1989) Pfluegers Arch. 423, 242–248.
55 Engel, A., Massalski, A., Schindler, H., Dorset, D.L. and Rosenbusch, J.P. (1985) Nature 317, 643–645.

* In fact in phylogenesis the need of saver and faster conduction required higher transmembrane current density. Increased conductivity per channel might result in loss of ionic selectivity. Increased density of monochannels is likely a more elaborate way than the establishment of oligochannels in concerted action. This may be a general concept to multiple efficacy of ion channels – as it is already established for many enzyme systems.